



## Co-occurrence patterns and assembly processes of microeukaryotic communities in a semi-enclosed aquaculture bay

Yifan Ma<sup>a,b,c</sup>, Yongbo Pan<sup>a,b,c</sup>, Qianqian Liu<sup>a,b,c</sup>, Lingfeng Huang<sup>d</sup>, Wenjing Zhang<sup>a,b,c,\*</sup>

<sup>a</sup> State Key Laboratory of Marine Environmental Science, Marine Biodiversity and Global Change Research Center, College of Ocean and Earth Sciences, Xiamen University, Xiamen, China

<sup>b</sup> Xiamen Key Laboratory of Urban Sea Ecological Conservation and Restoration, Xiamen University, Xiamen, China

<sup>c</sup> Fujian Key Laboratory of Coastal Pollution Prevention and Control, Xiamen University, Xiamen, China

<sup>d</sup> Key Laboratory of the Ministry of Education for Coastal and Wetland Ecosystems, College of the Environment and Ecology, Xiamen University, Xiamen, China

### ARTICLE INFO

#### Keywords:

Microeukaryotes  
Co-occurrence  
Community assembly  
Semi-enclosed bay  
Aquaculture

### ABSTRACT

Little was known about the biogeographical patterns, interaction and assembly processes of microeukaryotic communities in semi-enclosed aquaculture bays. Here, we examined microeukaryotic communities in 53 water samples from Sansha Bay (a typical semi-enclosed aquaculture bay), China. We found 9,282 operational taxonomic units (OTUs, 97% sequence identity), including 25 abundant OTUs and 8,919 rare OTUs. Ciliophora and Dinoflagellata were the most diverse and abundant lineages. (i) Although the degree of separation was different, both abundant and rare taxa showed significant separation between the three aquaculture areas (MAC, macroalgal culture; CAC, cage culture (*Larimichthys crocea*); and MIC, mixed culture) of the bay. Significant distance-decay relationships (DDRs) were found for both abundant and rare taxa in the bay, and the DDRs of rare taxa was stronger. Dispersal limitation was the main inducement to form this pattern. (ii) Co-occurrence network analysis revealed a complex interaction pattern dominated by cooperative relationships (84.15%). There were different ecological modules in the network, and they are closely related to different aquaculture areas. Aquaculture activities and taxonomic relatedness were important factors for the co-occurrence pattern of microeukaryotes. In addition, rare taxa enhanced the community habitat specificity and occupied most (71.3%) of the key nodes (including module hubs and connectors) in the network, suggesting that rare taxa played an important role in maintaining the stability of microeukaryotic community and co-occurrence pattern. (iii) Variation partitioning analysis (VPA) indicated that spatial factors exhibited greater influence on both abundant and rare taxa than environmental variables. More importantly, rare taxa was primarily governed by stochastic processes ( $NST_{jac} = 67.8\% \pm 1.9\%$ ), while deterministic processes played a decisive role in abundant taxa assembly ( $NST_{jac} = 21.5\% \pm 2.5\%$ ).

### 1. Introduction

Marine aquaculture is currently the fastest growing food industry worldwide (Gentry et al., 2017a; Ferreira et al., 2014). Coastal semi-enclosed bays with calm waters and convenient transportation make offshore aquaculture feasible (Gentry et al., 2017b), but these aquaculture zones are facing severe environmental and ecological challenges due to increased release of organic pollutants and land-based pollution, increased decomposition processes, resulting in nutrient-rich water (Farmaki et al., 2014). While microeukaryotes play pivotal roles in maintaining the health of the marine ecosystem (Anderson et al.,

2013; de Vargas et al., 2015), and they are crucial drivers of ecological functions and biogeochemical activities across ecosystems (including photosynthesis, trophic coupling and elemental transformations). In addition, microeukaryotic communities can also respond quickly to environmental changes. On the one hand, aquaculture activities can significantly affect the structure and function of microeukaryotic communities in semi-enclosed bays. For example, it has been found that salmon farming reduces the diversity of benthic foraminifera in coastal environments off the west coast of New Zealand (Pawlowski et al., 2014). On the other hand, variations in the community structure of microeukaryotes may affect other components of the aquatic food web,

\* Corresponding author. State Key Laboratory of Marine Environmental Science, Marine Biodiversity and Global Change Research Center, College of Ocean and Earth Sciences, Xiamen University, Xiamen, China.

E-mail address: [zhangwenjing@xmu.edu.cn](mailto:zhangwenjing@xmu.edu.cn) (W. Zhang).

<https://doi.org/10.1016/j.csr.2021.104550>

Received 3 April 2021; Received in revised form 23 August 2021; Accepted 27 August 2021

Available online 30 August 2021

0278-4343/© 2021 Elsevier Ltd. All rights reserved.

leading to changes in their distribution and abundance (Finlay and Esteban, 1998). Therefore, the study of microeukaryotic communities in semi-enclosed bay aquaculture zones is of great significance for healthy aquaculture activities. Given the taxonomic complexity of microeukaryotes, only relatively recent advances in DNA sequencing technologies have accelerated our understanding of the diversity and distribution patterns of these organisms (Santoferrara et al., 2020). However, little is known about microeukaryotic distribution patterns, co-occurrences relationships and assembly mechanisms of semi-enclosed aquaculture bays.

Interactions among microbial species (such as mutualism and competition) are fundamental components of the food webs and define the functioning of aquatic ecosystems (Feichtmayer et al., 2017). Therefore, the interpretation and prediction of interspecies interaction should be an important part of the study of microeukaryotic communities. Co-occurrence networks generated from microbial datasets using mathematical and statistical methods (e.g., correlation-based methods) (Faust et al., 2012) have provided the potential to explore interactions among different taxa. These methods have revealed many valuable findings, including co-occurrence patterns among microbes within or between ecosystems (Williams et al., 2014) and the contribution of specific taxa to biogeochemical processes (e.g. sinking of carbon from surface waters) (Faust et al., 2012). Part of co-occurrence networks are the so-called modules, which represent elementary units of any biological network, which are biologically important because they were generally considered to have relatively isolated taxonomic, evolutionary and functional characteristics. A more insightful analysis will use other types of data such as environmental conditions or functional characteristics, combined with module structure, to infer its ecological significance (Liu et al., 2019; Yan et al., 2019). This can help us form hypotheses about complex microbial interactions and co-occurrence patterns.

As the central challenge in microbial ecology, assembly mechanisms should not be neglected in the study of microeukaryotic community, especially in the semi-enclosed aquaculture bays where ecological pressure is high. Some studies have shown that stochastic processes (e.g., dispersal limitation and community drift) play a key role in determining microeukaryotic community assembly (Logares et al., 2018; Wu et al., 2018; Chen et al., 2019a). However, increasing studies indicate that microeukaryotic communities in enclosed aquaculture waters can be generally driven by deterministic processes, e.g., “top-down” (planktivorous fish can directly or indirectly influence microeukaryotic communities through trophic cascade effects) and “bottom-up” (low or high nitrogen and phosphorus addition can influence microeukaryotic communities) ways (Pawlowski et al., 2014; Matsuzaki et al., 2018; Zheng et al., 2020). Given the differences among habitats, knowledge from enclosed aquaculture waters may not be applicable in semi-enclosed aquaculture bays. Therefore, it is of great significance to understand the assembly mechanisms of microeukaryotic communities in semi-enclosed aquaculture bays.

In natural ecosystems, most microeukaryotic communities consist of a few abundant taxa and large number of rare taxa (Logares et al., 2014; Zhang et al., 2018). Abundant taxa are usually major contributors to ecosystem functions due to their high abundance (Kim et al., 2013). Rare taxa, instead, serve as nearly unlimited reservoirs of genetic and functional diversity, while also playing important ecological roles (Lynch et al., 2015). However, there are no previous studies on the abundant and rare taxa of microeukaryotes in semi-enclosed aquaculture bays.

Sansha Bay (Fujian Province, China) is a 714 km<sup>2</sup> semi-enclosed aquaculture bay connected to the East China Sea by only a narrow outlet (about 2.9 km wide). The bay is the largest spawning site for the large yellow croaker (*Larimichthys crocea*) in China and forms the largest cage culture base of this fish species in Fujian (Xue et al., 2018a). Millions of tons of feed are required annually to support the production of *L. crocea* in the bay, of which 5–10% is not utilized and end decomposed into organic and inorganic matter in the water column (Duan et al.,

2001). This leads to eutrophication and frequent occurrence of harmful algal blooms in the area (Ding et al., 2018; Chen et al., 2019b). To deal with the eutrophication resulting from cage cultures (*Larimichthys crocea*), a fish-algae mixed culture system was constructed in Sansha Bay. This system couples the cage culture (*Larimichthys crocea*) area with an adjacent macroalgal culture area, which developed rapidly from 2003 to 2016 (Wu et al., 2015; Wei et al., 2017). The production of macroalgal cultures, mainly *Gracilaria lemaneiformis* and *Laminaria japonica*, reached more than 80,000 tons in 2018, allowing to counteract the release of dissolved nutrients (Xie et al., 2020). Therefore, this system in Sansha Bay has huge economic and ecosystem service values.

This study investigates the distribution patterns, co-occurrence relationship and community assembly of microeukaryotic communities in Sansha Bay based on high-throughput sequencing of the 18S rRNA gene. Here, we hypothesize that (i) the community structure of microeukaryotes show significant differences among different aquaculture areas (CAC, MAC, MIC), and the distribution patterns of abundant and rare taxa are similar; (ii) microeukaryotic co-occurrence pattern is not affected by aquaculture activities, and rare taxa is crucial in maintaining the stability of the network in the semi-closed bay aquaculture areas; (iii) in the semi-closed bay aquaculture areas, stochastic processes dominate the assembly of abundant taxa, while deterministic processes dominate the assembly of rare taxa.

## 2. Materials and Methods

### 2.1. Study area, sampling and environmental factors

This study was conducted in Sansha Bay in January 2019 (Supplementary Table S1). Sampling area covered the macroalgae culture area (MAC), mixed culture areas (MIC), and cage culture (*Larimichthys crocea*) area (CAC) (Fig. 1). The detailed sample information was shown in Supplementary Table S1. In total, 53 surface (0.5 m), middle (6–16 m) and bottom (4–31 m) water samples were collected using Niskin bottles. The samples were transported to the laboratory and processed immediately. To minimize the interference of debris, mesoplankton and macroplankton for microeukaryotic community analyses, water samples were pre-filtered through a 200 µm sieve. Then, 1 L of water sample was filtered through 0.22 µm polycarbonate filters (47 mm diameter, Millipore, Billerica, MA, USA). The filters were stored at –80 °C until DNA extraction.

Water temperature, salinity and depth were measured in situ with conductivity–temperature–depth (CTD) oceanic profilers (AML Base X). Other chemical parameters, including pH, total nitrogen (TN), total inorganic nitrogen (TIN), nitrite (NO<sub>2</sub>-N), nitrate (NO<sub>3</sub>-N), ammonium (NH<sub>4</sub>-N), phosphate (PO<sub>4</sub>-P), total phosphorus (TP) and active silicon (DSi) were measured according to standard methods (Office of the State Oceanic Administration, 2006) (Supplementary Fig. S1).

### 2.2. DNA extraction, PCR and illumina sequencing

The extraction of DNA from filters was carried out using the Fast DNA spin kit for soil (BIO101 systems, MP Biomedicals, Solon, OH, USA) following the manufacturer's instructions. The primers 1380F (5'-CCCTGCCHTTGTACACAC-3') and 1510R (5'-CCTTCYGCAGGTT-CACCTAC-3') were used to amplify the hypervariable V9 region of the eukaryotic 18S rRNA gene (Amaral-Zettler et al., 2009). The PCR mixture contained 15 µl of Phusion Master Mix (New England Biolabs, Beverly, MA, USA), 0.2 µM of forward and reverse primers, and about 10 ng template DNA. PCR reactions included an initial denaturation at 94 °C for 5 min, followed by 30 cycles of 94 °C for 30 s, 57 °C for 30 s, 72 °C for 15 s, and a final extension at 72 °C for 10 min. Triplicate PCR products for each sample were pooled in equal quantity and purified using GeneJET Gel Extraction Kit (Thermo scientific, Hudson, NH, USA). Libraries were generated using the NEB Next Ultra DNA Library Prep Kit for Illumina (New England Biolabs, Beverly, MA, USA) following

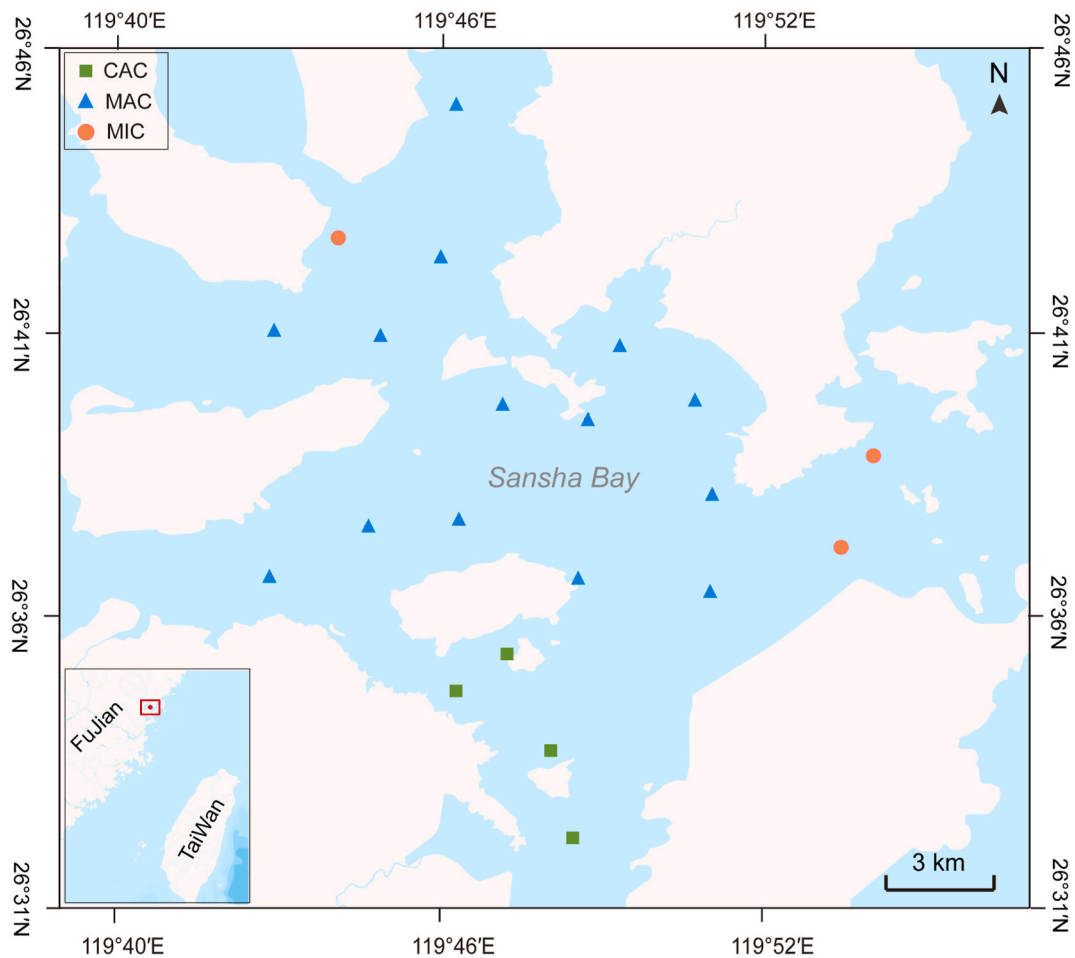


**Fig. 1.** Sampling sites across Sansha Bay and characteristics of aquaculture areas in the bay (B, C). MAC: macroalgal culture area; MIC: mixed culture area; CAC: cage culture area.

manufacturer's instructions, and barcode indexes were added. The library quality was assessed in the Agilent Bioanalyzer 2100 system (Agilent Technologies, Santa Clara, CA, USA). Finally, the libraries were sequenced on an Illumina X Ten platform (Illumina Inc., San Diego, CA, USA) using a paired-end ( $2 \times 150$  bp) approach (Caporaso et al., 2012).

### 2.3. Bioinformatics

Reads were merged with FLASH (Magoc and Salzberg, 2011). Raw data were analyzed and quality filtered in VSEARCH 1.9.1 (Rognes et al., 2016). The noise3 algorithm with default settings (minsize = 8) was used to denoise sequences. Before the downstream analyses, we used the uchime\_ref command to remove the chimeras. Quality filtered reads were then clustered into OTUs using the usearch\_global command at a 97% sequence similarity cutoff. Representative sequences from each OTU were aligned against the Protist Ribosomal Reference database (PR2 version 4.7.2) using the *sintra* algorithm (Guillou et al., 2013; Isabwe et al., 2019). Singleton OTUs were discarded before the downstream analyses due to potential sequencing errors. Before sample comparisons, the OTU table was randomly subsampled in MOTHUR v.1.33.3 (Schloss et al., 2009) to ensure an equal number of sequences (288,095) per sample.

### 2.4. Definition of OTUs based on relative abundance

OTUs were defined following recent publications (Mangot et al., 2013; Logares et al., 2014) as follows. Abundant OTUs (AT) presented relative abundance  $\geq 1\%$  in one or more samples (for each one), but

never  $< 0.01\%$  in each sample. Rare OTUs (RT) presented relative abundance  $< 0.01\%$  in one or more samples (for each one), but never  $> 1\%$  in each sample. Conditionally rare and abundant OTUs (CRAT) presented relative abundance  $\geq 1\%$  in some samples (for each one) and  $< 0.01\%$  in other samples (for each one). Moderately abundant OTUs (MT) presented relative abundance between 0.01 and 1% in each sample.

### 2.5. Community diversity and structure

Rarefaction curves and alpha diversity indices (ACE, Chao1, Shannon, Simpson and Pielou's evenness) were calculated in R v. 4.0.2 (R Core Team, 2015) using the Vegan package (Oksanen et al., 2019). Good's coverage was calculated in MOTHUR software v.1.33.3 software. Alpha-diversity was compared with one-way ANOVA in SPSS 20.0 (IBM Corp., Armonk, NY, USA). Heatmaps showing mean relative abundance and richness were generated with TTools (Chen et al., 2020). For exploration of distribution patterns in the bay, non-metric multidimensional scaling ordination (NMDS) analyses were conducted based on Bray-Curtis similarity. The analysis of similarity (ANOSIM) was used to test the significant differences in the community structure of different groups. Both NMDS and ANOSIM were conducted in PRIMER 7.0 (Clarke and Gorley, 2015).

### 2.6. Network analysis

An integrated co-occurrence network was constructed to assess the relationships among OTUs. To reduce noise and thus false-positive

predictions, OTUs presented in more than 17 samples (about 1/3 of all samples) and with more than 100 sequences were retained for the construction of networks (Liu et al., 2019). Pairwise Spearman's rank correlations ( $r$ ) between OTUs were calculated within the "psych" R package. Only robust and statistically significant ( $p$ -values  $< 0.01$  and  $|r| > 0.8$ ) correlations were included in the network analyses (Junker and Schreiber, 2008; Barberan et al., 2012). The correlation approach was justified by the analysis for the sampling effectuated according to Weiss et al. (2016). Network visualizations, node-level topological properties, and modular analysis were made with Gephi v. 0.9.2. The observed network was compared with 1000 Erdős-Rényi random networks, which were generated in the igraph R package and have an identical number of nodes and edges as the observed networks (R Core Team, 2015). Tukey's honest significance difference test was used to determine the statistical differences in node-level topological properties attributes across different taxa (All, AT, CRAT and MT). The nodes in the network can be classified into four subcategories by Zi-Pi plot, including peripherals ( $Z_i < 2.5$ ,  $P_i < 0.62$ ), connectors ( $Z_i < 2.5$ ,  $P_i \geq 0.62$ ), module hubs ( $Z_i \geq 2.5$ ,  $P_i < 0.62$ ) and network hubs ( $Z_i \geq 2.5$ ,  $P_i \geq 0.62$ ) (Guimera and Amaral, 2005).

### 2.7. Relationships between community composition, environmental variables, and geographical distance

Before multivariate statistical analyses, all environment variables except pH were  $\log(x+1)$  transformed to improve homoscedasticity and normality. According to the longitude and latitude coordinates of each sampling site, we calculated a geographical distance matrix. The links between the Bray-Curtis dissimilarity of community (square-root transformed abundances of OTUs) and geographical distances among sampling sites and Euclidean distance of environmental variables were determined using Spearman's rank correlations. Spatial variables (PCNM Nos. 1–8), the eigenvectors with associated positive eigenvalues extracted based on the longitude and latitude of sampling sites, were generated through coordinates of neighbor matrices (PCNM) analysis (Borcard and Legendre, 2002).

A redundancy analysis (RDA) was performed to explore the relationships between microeukaryotic communities and spatial, environmental variables, based on the longest gradient lengths of detrended correspondence analysis (DCA). Before the RDA analysis, the environmental and spatial variables with high variance inflation factor ( $VIF > 20$ ) were eliminated to avoid collinearity among factors, and the forward selection was conducted to select significant variables ( $p < 0.05$ ) using the "ordiR2step" function from the "vegan" package for downstream analyses (Blanchet et al., 2008). Then, variation partitioning analysis (VPA) with an adjusted  $R^2$  coefficient was performed to quantify the relative contribution of spatial factors (stochastic processes) and environmental selection in assembling communities (Wang et al., 2015).

### 2.8. Community assembly processes

To further disentangle the relative contributions of stochastic and deterministic processes on microeukaryotic community assembly, normalized stochasticity ratio (NST) index based on null model mathematical framework proposed by Ning et al. (2019) was used. NST (ranging from 0 to 100%) is an index developed with 50% as the boundary point, below the boundary point ( $NST < 50\%$ ) represents more deterministic assembly; above the boundary point ( $NST > 50\%$ ) denotes more stochastic assembly (Ning et al., 2019). Moreover, NST based on Jaccard distance ( $NST_{jac}$ ) was recommended to estimate the magnitude of stochastic assembly (Ning et al., 2019). We thus calculated NST variations based on Jaccard distance metrics using functions 'tNST' and 'nst.boot' in the "NST" package of R v. 4.0.2 (the parameters were as follows: "dist.method" = "jaccard," "abundance.weighted" = "TRUE", and "rand" = "1000").

## 3. Results

### 3.1. Distribution patterns of environmental variables in the bay

The distribution of environmental variables at the surface, middle and bottom layers of the bay were presented in Supplementary Fig. S1. In general, the distribution patterns of environmental factors among the three water layers were similar. Temperature decreased from the inside of the bay to the bay mouth, however, salinity showed an opposite trend. The analysis showed that the distribution patterns were similar for most of the nutrients factors ( $NO_3-N$ ,  $NO_2-N$ ,  $NH_4-N$ , TIN, TN, DSi and  $PO_4-P$ ) in the system. They were higher in the top of the bay, with lower concentrations observed near the bay mouth. Besides, the concentration of TP increased in the direction of the bay mouth.

### 3.2. Alpha diversity and community composition of microeukaryotes

In total, 9,282 microeukaryotic OTUs were identified from 15,269,035 high-quality reads clustered at a 97% identity level (Supplementary Table S2). In the whole dataset, 25 (0.33%) OTUs with 7,578,247 sequences (49.63%) were classified as abundant, whereas 8,919 (96.09%) OTUs with 1,779,543 (11.65%) sequences were classified as rare (Supplementary Table S2). The number of OTUs varied from 3,154 (sample 12A) to 4,117 (sample SFB) per sample (Supplementary Table S3). The rarefaction curves based on individual sample, samples from each of aquaculture areas and the pooled data (53 samples) all reach near saturation (Supplementary Fig. S2). Further, the total number of OTUs (9,282) was roughly equivalent to the number estimated by abundance-based richness estimators such as Chao1 ( $9,282 \pm 0.32$ ) and ACE ( $9,282 \pm 38$ ) (Supplementary Table S3). Good's coverage ranged from 99.57% to 99.65% in each sample and the index of all samples combined was 100% (Supplementary Table S3). The extrapolated richness indices, Good's coverage indices and rarefaction curves indicated that the sequencing depth was enough to recover most microeukaryote OTUs from the studied sites (Supplementary Table S2, Table S3 and Fig. S2).

A total of 2,612 OTUs (28.1%) could not be assigned to specific supergroups based on  $> 80\%$  sequence similarity and were lumped here as unclassified (Supplementary Table S4). The remaining 6,670 assignable OTUs (71.9%) were classified into 36 deep-branching lineages covering the full spectrum of cataloged eukaryotic diversity among seven recognized groups or supergroups (Adl et al., 2012; Guillou et al., 2013), namely Alveolata, Stramenopiles, Opisthokonta, Rhizaria, Archaeplastida, Excavata, Amoebozoa (according to the order of mean relative abundance), and multiple lineages of uncertain placement (Aposomonadidae, Centroheliozoa, Cryptophyta, Haptophyta, Katablepharidophyta, Picozoa and Telonemia; Supplementary Fig. S3, Table S4). Alveolata dominated the microeukaryotic community in terms of richness and abundance (21.1% OTUs and 44.6% sequences, respectively), followed by Stramenopiles (13.0% OTUs and 13.2% sequences, respectively) and Opisthokonta (17.4% OTUs and 8.3% sequences, respectively; Supplementary Table S4). Each of the 36 deep-branching sub-lineages was represented by more than 1,000 sequences. Three sub-lineages (Ciliophora, Dinoflagellata and Metazoa) were dominant in all three areas (MAC, CAC and MIC). Among these, Ciliophora (21.3–22.6% of sequences) and Dinoflagellata (19.4–22.5% of sequences) presented the highest relative abundances (Supplementary Fig. S3, Table S4). Six 'hyperdiverse' sub-lineages (Ciliophora, Dinoflagellata, Cercozoa, Chlorophyta, Fungi and Metazoa) each contained more than 4% of the OTUs richness, with Dinoflagellata (8.8–9.4% of OTUs) and Cercozoa (8.8–9.2% of OTUs) being the most diverse (Supplementary Fig. S3, Table S4).

### 3.3. Geographical patterns of microeukaryotic communities

The microeukaryotic communities in the three studied areas (MAC,

MIC and CAC) were significantly different (ANOSIM,  $p = 0.001$ ) based on all, abundant or rare OTUs (Fig. 2A, Table 1). However, in terms of vertical stratification, there was no significant separation among surface, middle and bottom communities ( $p > 0.05$ ; Fig. 2A, Table 1). Notably, the MAC and MIC communities were more similar to each other than to the other regions based on all, abundant or rare OTUs (Fig. 2A; Table 1). All abundant OTUs were shared in the three studied areas, while 69% and 67.4% OTUs were shared based on all and rare taxa, respectively (Fig. 2B).

Distance-decay relationship (DDR) analyses showed that the dissimilarity in microeukaryotic community composition between any two sample sites increased with geographical distance, with abundant OTUs displaying weaker DDRs compared to all or rare OTUs (Supplementary Fig. S4A). Instead, the community composition did not exhibit any significant relationship with the Euclidean distance based on environmental variables (Supplementary Fig. S4B). Neither there was a significant relationship between the Euclidean distances based on environmental variables and geographic distances (Supplementary Fig. S4C).

### 3.4. Co-occurrence network of microeukaryotic community

To discern co-occurrence patterns in the semi-enclosed aquaculture bay, a network was constructed based on OTU correlations (Fig. 3 A). The degrees of distribution fitted the power-law distribution very

**Table 1**

Analysis of similarities (ANOSIM) of microeukaryotic communities considering all, abundant or rare OTUs by aquaculture type and water layer. See also.

Pairwise tests	All		Abundant		Rare	
	R	P	R	P	R	P
MAC vs. MIC	0.318*	0.015	0.225*	0.040	0.301*	0.035
MAC vs. CAC	0.556**	0.001	0.278**	0.007	0.650**	0.001
CAC vs. MIC	0.668**	0.001	0.679**	0.001	0.383**	0.002
Global test	0.477**	0.001	0.302**	0.001	0.502**	0.001
Surface vs. Middle	-0.114	0.972	-0.069	0.823	-0.091	0.944
Surface vs. Bottom	-0.025	0.841	-0.009	0.515	-0.027	0.845
Bottom vs. Middle	-0.117	0.993	-0.057	0.806	-0.107	0.995
Global test	-0.068	0.994	-0.034	0.857	-0.06	0.994

Complete differentiation is indicated by  $R = 1$ , whereas  $R = 0$  suggests no differentiation among sample groups.

\* $p < 0.05$ .

\*\* $p < 0.01$ .

strongly ( $R^2 = 0.962$ , Supplementary Fig. S5), indicating meaningful and non-random associations in the network. The resulting network consisted of 4,452 edges connecting 517 nodes (Supplementary Table S5), with a much higher percentage of positive correlations (84.15%) observed than negative ones (15.85%). This suggested that facilitation, rather than competition, was more common within the community. These higher network indices (modularity, clustering coefficient, average path length and network diameter) for the observed

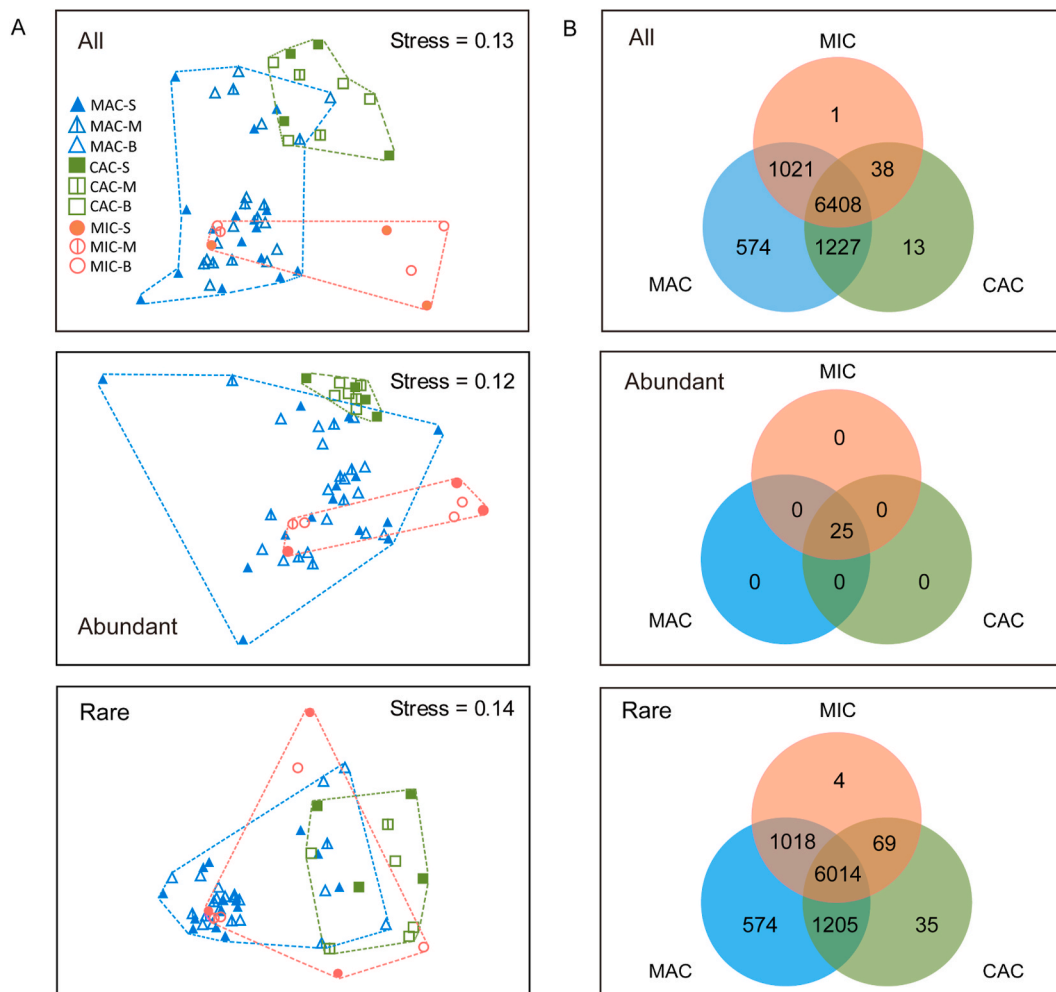


**Fig. 2.** Non-metric multidimensional scaling ordinations (nMDS) for microeukaryote communities from 53 samples (A) and Venn diagrams showing the numbers of unique and shared OTUs among the three sampling areas (B). MIC, mixed culture area; CAC, cage culture (*Larimichthys crocea*) area; MAC, macroalgal culture area; S, samples from surface water; M, samples from middle water; B, samples from bottom water.

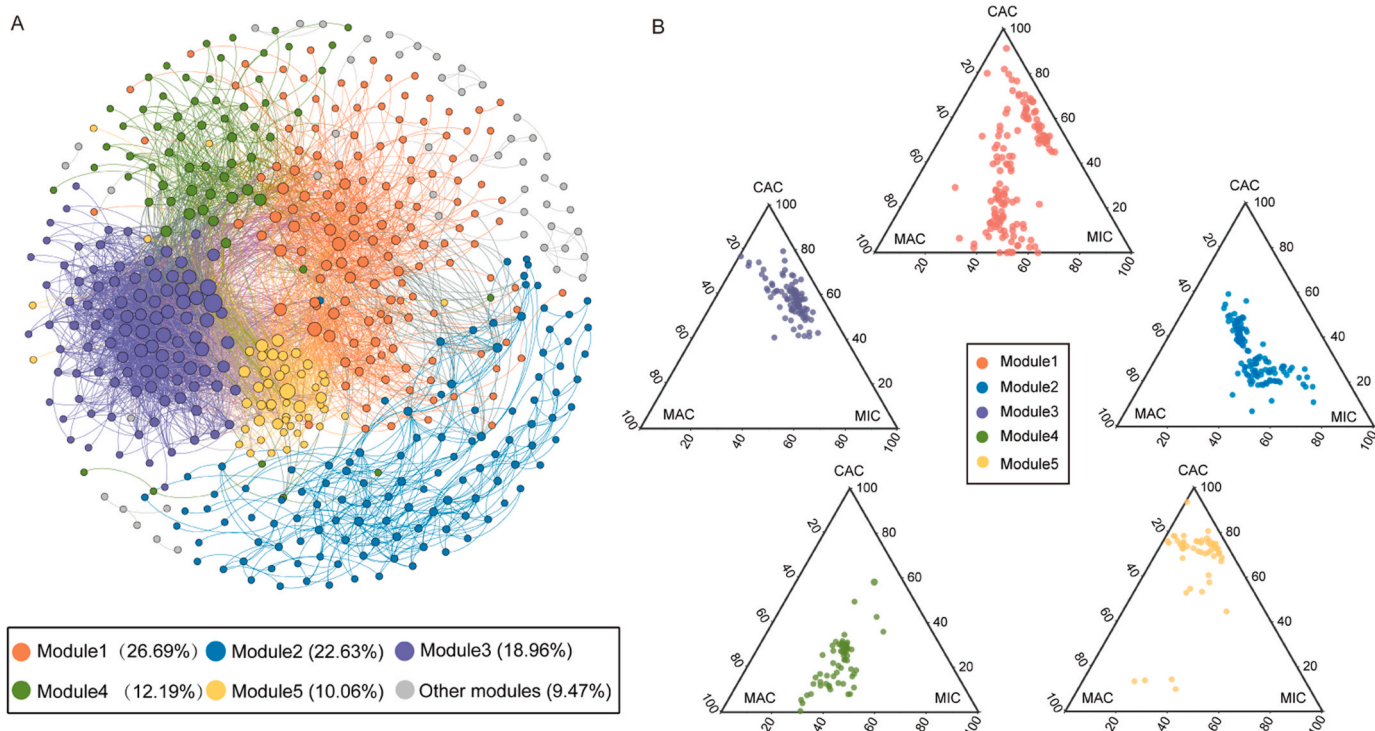


**Fig. 3.** Network analysis indicating co-occurrence patterns among OTUs. (A) The nodes were colored according to different modularity classes. (B) Ternary plots showing relative abundance of OTUs from modules 1–5 in the three different aquaculture areas. In (A), the size of each OTU is proportional to its number of connections. A connection stands for a strong (Spearman’s  $|r| > 0.8$ ) and significant ( $p < 0.01$ ) correlation. In (B) Each circle represented one individual OTU. For each OTU, abundance was averaged over all samples at each aquaculture area.

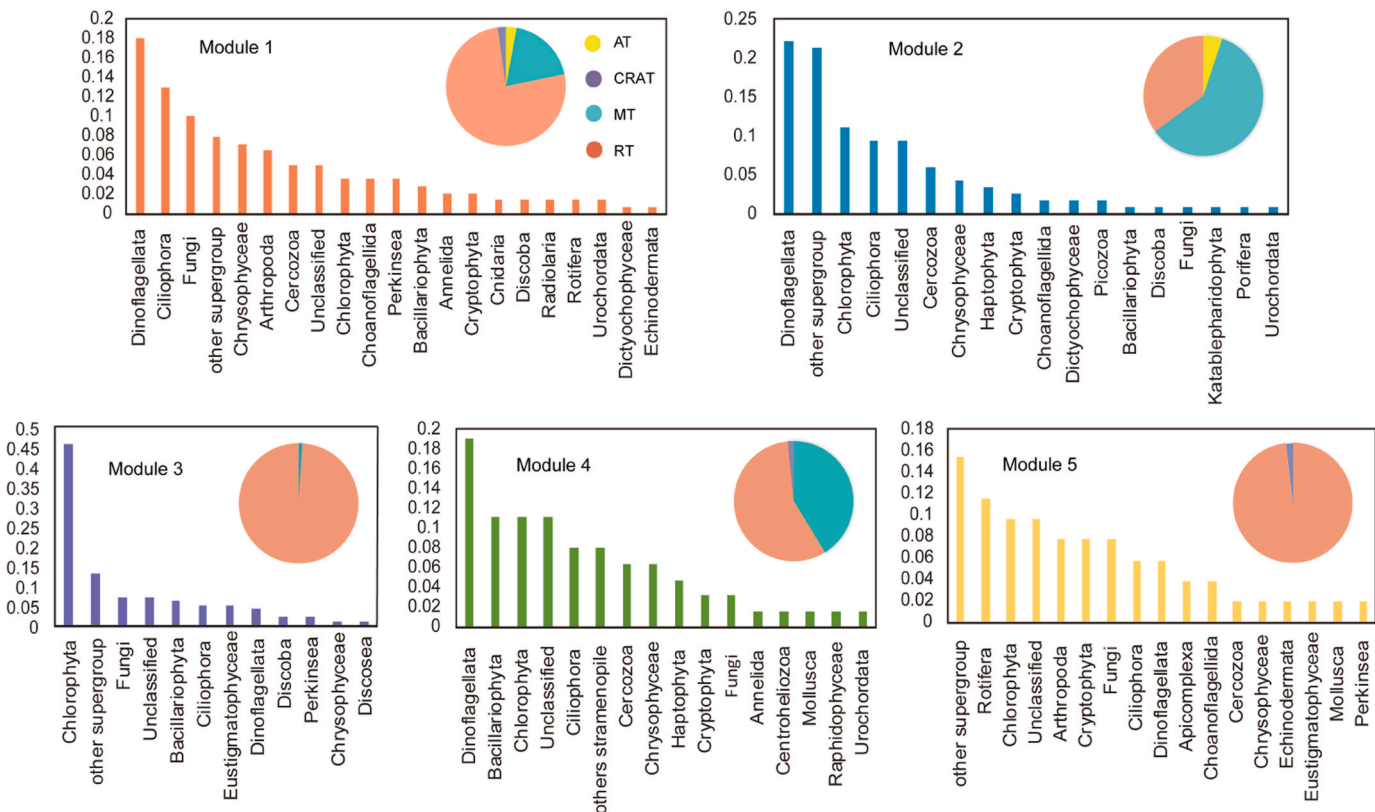


**Fig. 4.** Sub-community and taxonomic composition of major modules. AT, abundant OTUs; RT, rare OTUs; MT, moderately abundant OTUs; CRAT, conditionally rare and abundant OTUs.

network compared to random networks showed that the observed network had “small-world” properties (the fact that most pairs of nodes are connected by a relatively short path through the network) and modular structure (Supplementary Table S5). The proportion of rare taxa in the network reached 70.02%, while non-rare taxa frequently interacted more with rare taxa than with themselves (Supplementary Fig. S6). Node-level topological features of abundant, rare and other OTUs were also compared in our analysis. There are significant differences in betweenness centrality, degree and eigenvector centrality between moderate and rare OTUs. Both eigenvector centrality and degree of rare OTUs were significantly higher than those of moderate OTUs, while the betweenness centrality of moderate OTUs was significantly higher than that of rare OTUs. However, closeness centrality values showed no significant differences among the four subcommunities (Supplementary Fig. S7).

### 3.5. Modular structure of the Co-occurrence network

The integrated network was clearly parsed into 5 major modules, which accounted for the vast majority (90.53%) of the whole network (Fig. 3A). Ternary plot indicated that some modules were specific (relatively more abundant) to a particular region (MAC, MIC and CAC) (Fig. 3B). For example, most of the OTUs from module 3 and module 5 had higher relative abundances in CAC. Partial OTUs from Module 1 had relatively high abundance in CAC, suggesting that module 1 was partial-specific. However, the relative abundance of OTUs in module 2 and module 4 was basically the same among the three regions, indicating that module 2 and module 4 were common and non-specific in the whole region. These results indicated that aquaculture activities had a

significant effect on the microeukaryotes co-occurrence patterns. To further understand the modular structure in the network, we analyzed the taxonomic and OTU category (AT, RT, CRAT, MT) composition of different modules (Fig. 4). The nodes from module 1 mostly consisted of Dinoflagellata, Ciliophora, and Fungi. The nodes from module 2 mostly belonged to Dinoflagellata, Chlorophyta, and Ciliophora. While Chlorophyta accounts for nearly half of the nodes in module 3. The nodes from module 4 mostly consisted of Dinoflagellata, Bacillariophyta, and Chlorophyta. The node proportions of major taxa (Rotifera, Chlorophyta, Arthropoda, Cryptophyta and Fungi) in module 5 were generally low. Therefore, taxonomic relatedness was obviously a key factor in determining the modular structure. Interestingly, specific modules (module 3 and module 5) related to CAC were almost entirely composed of rare OTUs and rare OTUs also dominate in partial-specific module 1 (Fig. 4, Supplementary Table S6). Therefore, rare taxa played an important role in the formation of specific and partial-specific modules.

In addition, we counted the connections within and between modules (Fig. 5). There was the highest number of connections in module 3 and all of them were positively correlated (Fig. 5). Although the number of connections in module 5 was not high, the proportion of positive correlations was also nearly 99%. In module 1, module 2 and module 4, the internal positive correlations were also dominant, while the number of negative correlations cannot be ignored, especially in module 1 (26% negative correlations). These results indicated that all modules were dominated by favorable cooperation to play a specific function, among which the non-specific modules had relatively strong competition for resources. We found a relatively strong relationship among modules 1, 3 and 5. The number of negative correlations between module 1 and module 3 was slightly higher, the number of positive correlations

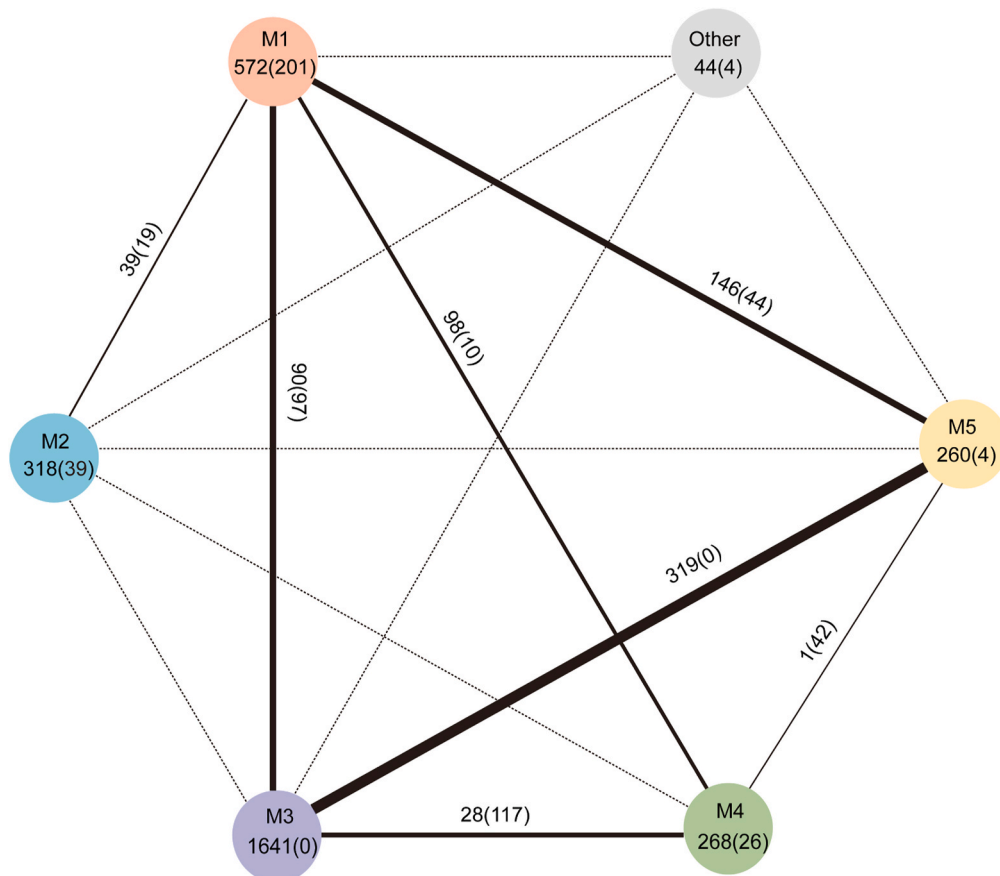


Fig. 5. The networks analysis showing the intra-associations within each module and inter-associations between different modules. A connection stands for a strong (Spearman's  $r > 0.8$  or  $r < -0.8$ ) and significant ( $P$ -value  $< 0.01$ ) correlation. Numbers outside and inside parentheses represent positive edge numbers and negative edge numbers, respectively. M1, module 1; M2, module 2; M3, module 3; M4, module 4; M5, module 5; Other, other modules.

between module 1 and module 5 was higher, and all relationships between module 3 and module 5 were positive. It was worth noting that the relationships between module 4 and specific modules (module 3 and module 5) were mainly negative. So, there might be a strong cooperative relationship between specific module 3 and module 5, to synergistically play ecological functions. However, there were strong competitive relationships between non-specific modules 4 and specific modules (module 3 and module 5). Partial-specific modules 1 showed different results in the interaction with specific modules 3 and 5, that was, the competitive effect was slightly stronger with module 3, and the cooperative relationship with module 5 was more significant.

Based on the connectivity of the OTUs shown as Zi-Pi plot, 2 and 78 OTUs were identified as module hubs and connectors in the network respectively (Supplementary Fig. S8, Supplementary Table S7). Both module hubs (*Ochrophyta* and Unclassified) were derived from module 2 and belonged to abundant OTUs. These connectors (including 57 rare OTUs, 17 moderately abundant OTUs, 3 conditionally rare and abundant OTUs and 1 abundant OTUs) mainly came from module 1, 4 and 5. Among these, Cercozoa, Chlorophyta, Ciliophora and Dinoflagellata were the dominant groups.

### 3.6. Shaping factors and assembly mechanisms of microeukaryotic community

The RDA showed that all, abundant and rare OTUs were significantly correlated with salinity and spatial variables (based on geographical distance), where the spatial variables were slightly different (Fig. 6A). For example, six spatial variables (PCNM Nos. 1–3, PCNM No. 5 and PCNM Nos. 7–8) were significantly correlated with all OTUs ( $p < 0.01$ , Fig. 6A); five spatial variables (PCNM Nos. 1–2, PCNM No. 5 and PCNM Nos. 7–8) were significantly correlated with the abundant OTUs ( $p < 0.01$ ; Fig. 6A); and five spatial variables (PCNM Nos. 1–3, PCNM No. 5 and PCNM Nos. 8) were significantly correlated with the rare OTUs ( $p <$

0.01, Fig. 6A). Variation partitioning analysis (VPA) indicated that spatial and environmental variables together explained 30%, 37% and 24% community variation of all, abundant and rare microeukaryotes, respectively (Fig. 6B). Among these, spatial factors independently explained 18%, 21% and 13% of community variation. However, the explained proportion of purely environmental factors for the three taxa was only 2%, 3% and 2%. A fairly large variation (70%, 63% and 76% for all, abundant and rare OTUs, respectively) was not explained by the spatial and environmental variables studied here.

In our study, both all and rare taxa showed similar community assembly process, while the abundant taxa showed the opposite assembly process (Table 2). The NST based on Jaccard distance ( $NST_{jac}$ ) index showed that all and rare community were predominately governed by stochastic processes ( $NST_{jac} = 83.6\% \pm 3.9\%$  for all community,  $NST_{jac} = 67.8\% \pm 1.9\%$  for rare community), while deterministic processes played a decisive role in controlling abundant community assemblages ( $21.5\% \pm 2.5\%$ ) (Table 2).

**Table 2**

Relative importance of ecological stochasticity in governing microeukaryotic community assembly estimated by the normalized stochasticity ratio (NST).

Taxa	NST (Jaccard dissimilarity)	Min	Quantile 25	Median	Quantile 75	Max
ALL	83.6% $\pm$ 3.9%	0.689	0.811	0.838	0.865	0.943
AT	21.5% $\pm$ 2.5%	0.142	0.197	0.214	0.231	0.32
RT	67.8% $\pm$ 1.9%	0.618	0.665	0.678	0.691	0.735

NST values are indicated by mean  $\pm$  standard deviation. NST <50% indicates more deterministic assembly.

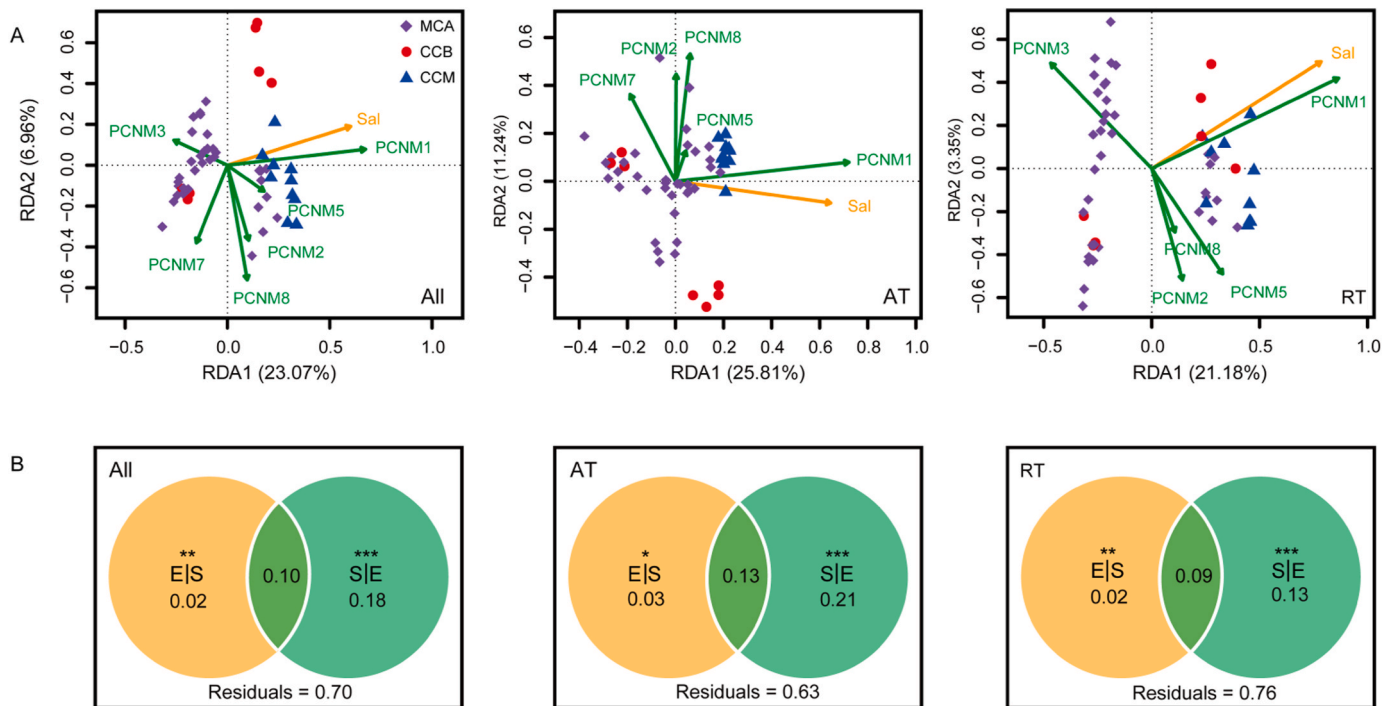


**Fig. 6.** Effects of environmental and spatial variables on microeukaryotic community composition. (A) RDA ordinations showing community composition in relation to significant environmental and spatial variables ( $p < 0.05$ ). Sal, salinity; PCNM, spatial variables (see Materials and Methods for definitions). Analyses were done separately for all (left), abundant (middle) and rare (right) OTUs. (B) Venn diagram of variation partitioning, showing the effects of spatial and environmental variables on the community composition. Values indicate the percentage of community variation explained by each fraction, including pure, shared, explained and unexplained variability. Forward selection procedures were used to select the best subset of spatial and environmental variables explaining community variation, respectively. \*\*\* $p < 0.001$ , \*\* $p < 0.01$ , \* $p < 0.05$ .

## 4. Discussion

### 4.1. Community composition of microeukaryotes

Alveolata, Stramenopiles and Opisthokonta were the main supergroups in the Sansha bay (Supplementary Fig. S3, Table S4). At a more refined taxonomic level, we found that ciliates (22% of total abundance) and dinoflagellates (22% of total abundance) were the dominant lineages of Alveolata and the whole community (Supplementary Fig. S3, Table S4). The dominance of dinoflagellates was consistent with the results obtained by Song et al. (2016) in the coastal shellfish culture areas of Qinhuangdao, while they found that dinoflagellates accounted for 54% of the total abundance and pelagomonadales for 40% of the total abundance. These different results might be due to the difference in the research focus: Song et al. (2016) focused on picoeukaryotes (2–3  $\mu\text{m}$ ), while our research targeted microeukaryotes (0.22  $\mu\text{m}$ –200  $\mu\text{m}$ ). Secondly, the differences might be due to the influence of different aquaculture types. Thirdly, the rDNA copy numbers in molecular sequencing methods might lead to biased relative abundances (Gong et al., 2015; Santoferrara, 2019). Stramenopiles was the second supergroup in terms of relative abundance, represented mainly by Bacillariophyta (Supplementary Fig. S3, Table S4), which was a dominant lineage in many ecosystems. On the one hand, Bacillariophyta played a great role in ecological processes and aquatic food webs (Menden-Deuer and Lessard, 2000; Agusti et al., 2015). On the other hand, Bacillariophyta (e.g. *Skeletonema costatum*) could also trigger harmful algal blooms that can seriously affect aquaculture development and human health (Moore et al., 2008). Based on mean relative abundance, Opisthokonta was the third largest group of planktonic microeukaryotes (Supplementary Fig. S3, Table S4). This included mostly metazoans and fungi, even if a 200  $\mu\text{m}$  pore-size sieve was used to remove large organisms. The presence of smaller life stages (eggs or larvae) of large-sized organisms might contribute to the assemblage (Liu et al., 2017). Interestingly, the phenomenon of high diversity but low abundance appeared in metazoan and fungi (Supplementary Fig. S3, Table S4). The result was consistent with previous studies in surface marine waters (Massana and Pedro-Alio, 2008) and deep anoxic waters (Edgcomb et al., 2011). This high diversity/low abundance pattern might be linked to high dispersal of Opisthokonta cells or stages (e.g., fungal spores), which resulted in their ubiquitous distribution (Zhang et al., 2018).

### 4.2. Distribution patterns of abundant and rare taxa

Microeukaryotic assemblages (AT and RT) were clearly separated among the three aquaculture areas (CAC, MIC and MAC; Fig. 2A), while sampling depth (surface, middle and bottom) had no significant effect on the communities (Fig. 2A, Table 1). These results implying a strong influence of vertical mixing (especially since our sampling occurred in winter) or sinking of organisms from upper to lower water layers (Zhang et al., 2014). Compared to bacteria, we known less about the distribution patterns of abundant and rare marine microeukaryotic taxa, and there was still insufficient exploration of the diversity of marine microeukaryotes (Logares et al., 2014). In our study, the distribution pattern of abundant taxa was slightly different compared to that for rare taxa. These differences were mainly reflected in the biodiversity pattern and distance-decay relationship (Fig. 2B, Supplementary Fig. S4 and Table 2), i.e. abundant taxa had weaker distance-decay relationships and higher shared OTU ratio (between aquaculture areas) than rare taxa. As we all known, dispersal limitation of microeukaryotes could lead to a decrease in community similarity, as individuals were more likely to colonize nearby than distant habitats (Lear et al., 2014). Moreover, unlike previous studies which found that environmental selection could also lead to distance-decay of community similarity (Hanson et al., 2012), this phenomenon did not exist in our study. Because, there was no significant increase in Euclidean distance with geographical distance,

and there was also no significant correlation between Euclidean distance and community dissimilarity (Supplementary Fig. S4). Therefore, above differences might be due to the weaker response to dispersal limitations exhibited in abundant taxa than in rare taxa, that was, abundant taxa had stronger dispersal ability. Our result further reinforced the idea that homogenizing dispersal dominates at small spatial scales, leading to community dissimilarity at closely located sites (Feng et al., 2019).

### 4.3. The general co-occurrence patterns of microeukaryotes

In our study, the observed network had power-law distribution, non-random and modular structure properties (Supplementary Fig. S5), which might reflect competitive or cooperative interactions and niche differentiation, thus leading to the complexity of co-occurrence network (Olesen et al., 2007). The positive correlation was mainly regarded as cooperation in the network (Ju et al., 2014), and about 84% positive correlations were observed in the observed network. Notably, the positive correlations between rare taxa and non-rare taxa were much more than the negative ones (Supplementary Fig. S6). Previous studies had reported that the cooperation between rare and non-rare microbial taxa could provide a buffer against environmental disturbance (Konopka et al., 2015) and support ecosystem function and stability (Ziegler et al., 2018). Therefore, the cooperation between rare and non-rare taxa in our network might contribute to the stability of microeukaryotic communities in the semi-enclosed aquaculture bay. Further analysis of network topology characteristics indicated that 73% of all connectors belonged to rare OTUs (Supplementary Table S7), again highlighting the importance of rare taxa in maintaining the stability of the microeukaryotic community and co-occurrence patterns (Xue et al., 2018b).

### 4.4. Structure characters of the network modules

We explored the module structure of co-occurrence networks and the nodes were clustered into five major modules (Fig. 3A). As described in previous study (Olesen et al., 2007), modularity might reflect clustering of taxonomically related species, as we found that each module was dominated by several dominant taxa (Fig. 4). Module 3 and module 5 showed significant region specificities related to CAC, module 1 showed partial region specificities related to CAC, while module 2 and module 4 did not (Fig. 3B). These results providing evidence for the relationship between different habitat characteristics and module composition. Some studies have interpreted modules as ecological niches (Williams et al., 2014), and taxa within the same module may perform similar or complementary functions (Xiong et al., 2018). For instance, module 3 was dominated by Chlorophyta (Fig. 4). Yokoyama and Ishihi (2010) found that Chlorophyta could act as a suitable bioindicator and biofilter for dissolved inorganic nitrogen derived from coastal fish farms. Therefore, module 3 might play a key role in the absorption of DIN produced by cage culture (*Larimichthys crocea*). In addition, Chlorophyta could also provide essential fatty acids, pigments, amino acids and vitamins for farmed fish (Santhanam et al., 2015). Rotifera was the most abundant taxa in module 5 (specific to CCA) (Fig. 4). These organisms played a crucial role in the coastal aquaculture of fish, especially in meeting the nutritional requirements of fish larvae (Santhanam et al., 2015).

There were also complex interactions between modules (Fig. 5), which might be determined by the functions performed by these modules. For example, the dominant taxa in Module 3 (Chlorophyta) and Module 5 (Rotifera) were all important food for fish larvae, and there were significant positive correlations between the two modules. This suggested that there might be a degree of cooperation between two functionally similar modules in the semi-closed aquaculture bay we studied. Modules 1, 2 and 4 were mainly composed of rare OTUs and moderately abundant OTUs (Supplementary Table S6), while Modules 3 and 5 were almost entirely composed of rare OTUs and showed significant specificity for CAC (Fig. 4). These results indicated that the proportion of rare taxa played an important role in the habitat specificity of

the module. Yao et al. (2020) had found a similar conclusion in forest communities that an increase in the proportion of rare species increases the ecological specificity of the community under a given total abundance.

#### 4.5. Factors and controlling mechanisms shaping the microeukaryotic plankton community

Understanding the mechanisms that generate and maintain microbial diversity is an important aspect of microbial ecology (Hanson et al., 2012). This study revealed that both environmental (salinity) and spatial variables (based on geographical distance) played a simultaneous role in the assembly of microeukaryotic community in the semi-enclosed aquaculture bay (Fig. 6). Stochastic processes played a leading role in the construction of total and rare communities, while deterministic processes played a leading role in the construction of abundant community (Table 2).

On one hand, salinity was the most important environmental factor that was significantly related to the community composition of all three taxa (all, abundant and rare taxa, Fig. 6A). As a major environmental variable across many ecosystems at the local-scale and continental-scale, salinity has been reported to drive microbial community assembly strongly (Zhang et al., 2017; Santoferrara et al., 2018). For example, changes in planktonic ciliate diversity from inshore to offshore on the continental shelf and from shallow to deep waters were significantly associated with a modest increase in salinity (Grattepanche et al., 2016). On the other hand, spatial variables (based on geographical distance) known to influence microbial community assembly (Hanson et al., 2012) were significant in shaping microeukaryotic communities (all, abundant and rare taxa) in the bay (Fig. 6A). Even if both environmental selection (salinity) and spatial factors influenced community structure, our results indicated that environmental selection (salinity) played a smaller role in shaping the communities (VPA analysis; Fig. 6B). Unfortunately, the relationships between these parameters (salinity and spatial factors) and different aquaculture types were not clear, and there was a lack of collection of environmental parameters that were clearly associated with aquaculture. Therefore, the response of the microeukaryotic community in this semi-enclosed aquaculture bay to the change of aquaculture types was still cannot be understood fully. In comparison with other habitats, we found that this was consistent with previous studies on microbial communities in lakes and intertidal sediments (Yang et al., 2016; Pan et al., 2019), but not with analyses in Antarctica coastal lakes that evidenced a strong influence of environmental selection on microbial community composition (Logares et al., 2013). Differences in spatial scale and environmental gradients among study sites might explain this disagreement. Moreover, heterogeneous influence of environmental and spatial factors on the distribution of all, abundant or rare OTUs might be ascribed to specific properties of different taxa (Chen et al., 2017). In aquatic ecosystems, microbial properties such as physiological tolerance, dispersal capacity, taxonomic and functional diversity mediated the responses of communities to environmental and spatial changes (Gong et al., 2015; Liu et al., 2015).

There was a growing understanding of the mechanism of microeukaryotic community assembly, mainly focusing on two complementary processes, deterministic processes and stochastic processes (Chen et al., 2019a; Kong et al., 2019). We found that stochastic processes played a dominant role in the assembly of all and rare microeukaryotic community in the semi-enclosed aquaculture bay (Table 2). However, the assembly of abundant community was dominated by deterministic processes in this bay. In the preceding results, we had found that the microeukaryotic community in this bay has dispersal limitations (Supplementary Fig. S4, Fig. 6A). However, it was not clear whether dispersal was a stochastic process or a deterministic process (Vellend et al., 2014). Of course, if the dispersal rate depended on the size of population, it could be considered as a stochastic process (Zhou and

Ning, 2017). In our study, abundant taxa had significantly higher probability of dispersal than rare taxa, which not only showed that the dispersal rate depends on the population size, but also further proved the idea of stochasticity of dispersal. Therefore, it was not surprising that the rare taxa (which was more affected by dispersal limitations) was more influenced by stochastic process.

Moreover, recent studies have shown that deterministic and stochastic processes have different relative effects on microbial community assembly, depending on the geographic scale and intensity of environmental gradient (Hanson et al., 2012; Morrison-Whittle et al., 2015). Therefore, our conclusions might not be applicable to some different habitats (Wu et al., 2017). Although the  $NST_{jac}$  successfully predicted the microeukaryotic community assembly patterns in the bay, this was still insufficient to fully understand the large proportion of unexplained variance revealed by the VPA analysis (Fig. 6B). The unexplained variation might come from biotic interactions such as competition (Stegen et al., 2013), environmental factors we did not measure (e.g. tides, upwelling and the movement of currents), methodological limitations (Bahram et al., 2016) or stochastic processes of growth, death, colonization and extinction (Hanson et al., 2012). To better understand the assembly patterns of microeukaryotic communities in the semi-enclosed aquaculture bay, future studies should consider temporal variations, additional deterministic factors (e.g., unmeasured environmental factors and species interactions), and other possible stochastic factors.

## 5. Conclusion

This study provided insights for explaining microeukaryotic community geographical patterns, co-occurrence relationship and assembly mechanism in a semi-enclosed aquaculture bay for both abundant and rare taxa. The diversity and distribution patterns of abundant and rare taxa were different. On the one hand, abundant and rare taxa showed different degrees of separation between different culture areas of the bay. On the other hand, both groups of OTUs showed obvious DDRs, and the DDRs of rare taxa was stronger. The co-occurrence pattern of microeukaryotes suggested a prevalence of cooperative relationships, in which different ecological modules are closely associated with different aquaculture areas. The presence of rare taxa possibly enhanced the habitat specificity of microeukaryotic communities at small geographic scales, and probably played an important role in maintaining the stability of communities through synergistic effects with non-rare taxa. Spatial variables based on geographical distance explained more community variation in both abundant and rare taxa than non-biological environmental variables collected in this semi-enclosed aquaculture bay. The results based on  $NST_{jac}$  showed that the rare community assembly was primarily governed by stochastic processes, and the abundant one was primarily governed by deterministic processes. Overall, this study highlighted the important ecological significance of rare microeukaryotes in semi-closed aquaculture bays and further deepened the understanding of interactions among microeukaryotes and assembly mechanisms.

### Author contributions

WZ conceived the idea and designed the experiment process. LH, WZ, YM and QL organized the cruise and sample collection. YM carried the experiment. YM and WZ wrote the paper. YP and YM contributed to data elaboration. All authors contributed experimental assistance and intellectual input to this study.

### Data availability statement

All raw sequences from this study have been submitted to the NCBI Sequence Read Archive (SRA) database under the BioProject number PRJNA747143 and the accession number SRP328880. Detailed SRR accession numbers: SRR15185929, SRR15185928, SRR15185831,

SRR15185820,SRR15185873,SRR15185862,SRR15185851,  
SRR15185808,SRR15185797,SRR15185925,SRR15185927,  
SRR15185905,SRR15185894,SRR15185883,SRR15185840,  
SRR15185836,SRR15185835,SRR15185834,SRR15185833,  
SRR15185832,SRR15185830,SRR15185829,SRR15185828,  
SRR15185827,SRR15185826,SRR15185825,SRR15185824,  
SRR15185823,SRR15185822,SRR15185821,SRR15185819,  
SRR15185882,SRR15185881,SRR15185880,SRR15185879,  
SRR15185878,SRR15185877,SRR15185876,SRR15185875,  
SRR15185874,SRR15185872,SRR15185871,SRR15185870,  
SRR15185869,SRR15185868,SRR15185867,SRR15185866,  
SRR15185865,SRR15185864,SRR15185863,SRR15185861,  
SRR15185860,SRR15185859.

## Funding

This work was funded by the National Key Research and Development Program of China (2018YFC1406306) and the National Natural Science Foundation of China (42176147).

## Declaration of competing interest

The authors declare that they have no known competing financial interests or personal relationships that could have appeared to influence the work reported in this paper.

## Acknowledgments

We thank Prof. Jianyu Hu (Xiamen University) for providing CTD data. We thank Dr. Peng Xiao for the data processing. Dr. Luciana Santoferrara (University of Connecticut) provided comments on earlier versions of this manuscript.

## Appendix A. Supplementary data

Supplementary data to this article can be found online at <https://doi.org/10.1016/j.csr.2021.104550>.

## References

- Adl, S.M., Simpson, A.G., Lane, C.E., Lukes, J., Bass, D., Bowser, S.S., et al., 2012. The revised classification of eukaryotes. *J. Eukaryot. Microbiol.* 59 (5), 429–493. <https://doi.org/10.1111/j.1550-7408.2012.00644.x>.
- Agusti, S., Gonzalez-Gordillo, J.I., Vaque, D., Estrada, M., Cerezo, M.I., Salazar, G., et al., 2015. Ubiquitous healthy diatoms in the deep sea confirm deep carbon injection by the biological pump. *Nat. Commun.* 6. ARTN 760810.1038/ncomms8608.
- Amaral-Zettler, L.A., McCliment, E.A., Ducklow, H.W., Huse, S.M., 2009. A method for studying protistan diversity using massively parallel sequencing of V9 hypervariable regions of small-subunit ribosomal RNA genes. *PLoS One* 4 (7). ARTN e637210.1371/journal.pone.0006372.
- Anderson, R., Wylezich, C., Glaubitz, S., Labrenz, M., Jurgens, K., 2013. Impact of protist grazing on a key bacterial group for biogeochemical cycling in Baltic Sea pelagic oxic/anoxic interfaces. *Environ. Microbiol.* 15 (5), 1580–1594. <https://doi.org/10.1111/1462-2920.12078>.
- Bahram, M., Kohout, P., Anslan, S., Harend, H., Abarenkov, K., Tedersoo, L., 2016. Stochastic distribution of small soil eukaryotes resulting from high dispersal and drift in a local environment. *ISME J.* 10 (4), 885–896. <https://doi.org/10.1038/ismej.2015.164>.
- Barberan, A., Bates, S.T., Casamayor, E.O., Fierer, N., 2012. Using network analysis to explore co-occurrence patterns in soil microbial communities. *ISME J.* 6 (2), 343–351. <https://doi.org/10.1038/ismej.2011.119>.
- Blanchet, F.G., Legendre, P., Borcard, D., 2008. Forward selection of explanatory variables. *Ecology* 89 (9), 2623–2632. <https://doi.org/10.1890/07-0986.1>.
- Borcard, D., Legendre, P., 2002. All-scale spatial analysis of ecological data by means of principal coordinates of neighbour matrices. *Ecol. Model.* 153 (1–2), 51–68. Pii S0304-3800(01)00501-4Doi 10.1016/S0304-3800(01)00501-4.
- Caporaso, J.G., Lauber, C.L., Walters, W.A., Berg-Lyons, D., Huntley, J., Fierer, N., et al., 2012. Ultra-high-throughput microbial community analysis on the Illumina HiSeq and MiSeq platforms. *ISME J.* 6 (8), 1621–1624. <https://doi.org/10.1038/ismej.2012.8>.
- Chen, W., Pan, Y., Yu, L., Yang, J., Zhang, W., 2017. Patterns and processes in marine microeukaryotic community biogeography from Xiamen coastal waters and intertidal sediments, southeast China. *Front. Microbiol.* 8, 1912. <https://doi.org/10.3389/fmicb.2017.01912>.
- Chen, W., Ren, K., Isabwe, A., Chen, H., Liu, M., Yang, J., 2019a. Stochastic processes shape microeukaryotic community assembly in a subtropical river across wet and dry seasons. *Microbiome* 7 (1), 138. <https://doi.org/10.1186/s40168-019-0749-8>.
- Chen, Y.Z., Wang, Y.S., Xie, T.T., Zhang, M.H., 2019b. Analysis for the Change of Aquaculture Area and Water Quality in Sansha Bay during 2010-2018, 2019 Ieee International Geoscience and Remote Sensing Symposium (Igarss 2019), pp. 8264–8267.
- Chen, C.J., Chen, H., Zhang, Y., Thomas, H.R., Frank, M.H., He, Y.H., et al., 2020. TBools: an integrative toolkit developed for interactive analyses of big biological data. *Mol. Plant* 13 (8), 1194–1202. <https://doi.org/10.1016/j.molp.2020.06.009>.
- Clarke, K.R., Gorley, R.N., 2015. PRIMER V7: User Manual/tutorial. PRIMER-E, Plymouth, UK.
- de Vargas, C., Audic, S., Henry, N., Decelle, J., Mahe, F., Logares, R., et al., 2015. Eukaryotic plankton diversity in the sunlit ocean. *Science* 348 (6237). <https://doi.org/10.1126/science.1261605>.
- Ding, G.M., Zhang, S.F., 2018. Ecological characteristics and the causes of Karenia mikimotoi bloom in the Sansha Bay in 2012. *Hai Yang Xue Bao* 40 (6), 104–112. <https://doi.org/10.3969/j.issn.0253-4193.2018.06.010>.
- Duan, Q.Y., Mai, K.S., Zhong, H.Y., Si, L.G., Wang, X.Q., 2001. Studies on the nutrition of the large yellow croaker, *Pseudosciaena crocea* R. I: growth response to graded levels of dietary protein and lipid. *Aquacult. Res.* 32, 46–52. <https://doi.org/10.1046/j.1355-557x.2001.00048.x>.
- Edgcomb, V., Orsi, W., Bunge, J., Jeon, S., Christen, R., Leslin, C., et al., 2011. Protistan microbial observatory in the Cariaco Basin, Caribbean. I. Pyrosequencing vs Sanger insights into species richness. *ISME J.* 5 (8), 1344–1356. <https://doi.org/10.1038/ismej.2011.6>.
- Farmaki, E.G., Thomaidis, N.S., Pasiadis, I.N., Baulard, C., Papaharisis, L., Efstathiou, C.E., 2014. Environmental impact of intensive aquaculture: investigation on the accumulation of metals and nutrients in marine sediments of Greece. *Sci. Total Environ.* 485, 554–562. <https://doi.org/10.1016/j.scitotenv.2014.03.125>.
- Faust, K., Sathirapongsasuti, J.F., Izard, J., Segata, N., Gevers, D., Raes, J., et al., 2012. Microbial Co-occurrence relationships in the human microbiome. *PLoS Comput. Biol.* 8 (7). ARTN e100260610.1371/journal.pcbi.1002606.
- Feichtmayer, J., Deng, L., Griebler, C., 2017. Antagonistic microbial interactions: contributions and potential applications for controlling pathogens in the aquatic systems. *Front. Microbiol.* 8. ARTN 219210.3389/fmicb.2017.02192.
- Fen, M.M., Tripathi, B.M., Shi, Y., Adams, J.M., Zhu, Y.G., Chu, H.Y., 2019. Interpreting distance-decay pattern of soil bacteria via quantifying the assembly processes at multiple spatial scales. *Microbiologypopen* 8 (9). ARTN e85110.1002/mbo3.851.
- Ferreira, J.G., Saurel, C., Silva, J.D.L.E., Nunes, J.P., Vazquez, F., 2014. Modelling of interactions between inshore and offshore aquaculture. *Aquaculture* 426, 154–164. <https://doi.org/10.1016/j.aquaculture.2014.01.030>.
- Finlay, B.J., Esteban, G.F., 1998. Freshwater protozoa: biodiversity and ecological function. *Biodivers. Conserv.* 7 (9), 1163–1186. <https://doi.org/10.1023/A:1008879616066>.
- Gentry, R.R., Froehlich, H.E., Grimm, D., Kareiva, P., Parke, M., Rust, M., et al., 2017a. Mapping the global potential for marine aquaculture. *Nature Ecology & Evolution* 1 (9), 1317–1324. <https://doi.org/10.1038/s41559-017-0257-9>.
- Gentry, R.R., Lester, S.E., Kappel, C.V., White, C., Bell, T.W., Stevens, J., et al., 2017b. Offshore aquaculture: spatial planning principles for sustainable development. *Ecology and Evolution* 7 (2), 733–743. <https://doi.org/10.1002/ece3.2637>.
- Gong, J., Shi, F., Ma, B., Dong, J., Pachiadaki, M., Zhang, X.L., et al., 2015. Depth shapes alpha- and beta-diversities of microbial eukaryotes in surficial sediments of coastal ecosystems. *Environ. Microbiol.* 17 (10), 3722–3737. <https://doi.org/10.1111/1462-2920.12763>.
- Grattepance, J.D., Santoferrara, L.F., McManus, G.B., Katz, L.A., 2016. Unexpected biodiversity of ciliates in marine samples from below the photic zone. *Mol. Ecol.* 25 (16), 3987–4000. <https://doi.org/10.1111/mec.13745>.
- Guillou, L., Bachar, D., Audic, S., Bass, D., Berney, C., Bittner, L., et al., 2013. The Protist Ribosomal Reference database (PR2): a catalog of unicellular eukaryote Small Sub-Unit rRNA sequences with curated taxonomy. *Nucleic Acids Res.* 41 (D1), D597–D604. <https://doi.org/10.1093/nar/gks1160>.
- Guimera, R., Amaral, L.A.N., 2005. Functional cartography of complex metabolic networks. *Nature* 433 (7028), 895–900. <https://doi.org/10.1038/nature03288>.
- Hanson, C.A., Fuhrman, J.A., Horner-Devine, M.C., Martiny, J.B.H., 2012. Beyond biogeographic patterns: processes shaping the microbial landscape. *Nat. Rev. Microbiol.* 10 (7), 497–506. <https://doi.org/10.1038/nrmicro2795>.
- Isabwe, A., Ren, K.X., Wang, Y.M., Peng, F., Chen, H.H., Yang, J., 2019. Community assembly mechanisms underlying the core and random bacterioplankton and microeukaryotes in a river-reservoir system. *Water* 11 (6). <https://doi.org/10.3390/w11061127>.
- Ju, F., Xia, Y., Guo, F., Wang, Z., Zhang, T., 2014. Taxonomic relatedness shapes bacterial assembly in activated sludge of globally distributed wastewater treatment plants. *Environ. Microbiol.* 16 (8), 2421–2432. <https://doi.org/10.1111/1462-2920.12355>.
- Junker, B.H., Schreiber, F., 2008. *Analysis of Biological Networks*. Wiley Interscience, New York. Google Scholar.
- Kim, T.S., Jeong, J.Y., Wells, G.F., Park, H.D., 2013. General and rare bacterial taxa demonstrating different temporal dynamic patterns in an activated sludge bioreactor. *Appl. Microbiol. Biotechnol.* 97 (4), 1755–1765. <https://doi.org/10.1007/s00253-012-4002-7>.
- Kong, J., Wang, Y., Warren, A., Huang, B., Sun, P., 2019. Diversity distribution and assembly mechanisms of planktonic and benthic microeukaryote communities in intertidal zones of southeast fujian, China. *Front. Microbiol.* 10, 2640. <https://doi.org/10.3389/fmicb.2019.02640>.

- Konopka, A., Lindemann, S., Fredrickson, J., 2015. Dynamics in microbial communities: unraveling mechanisms to identify principles. *ISME J.* 9 (7), 1488–1495. <https://doi.org/10.1038/ismej.2014.251>.
- Lear, G., Bellamy, J., Case, B.S., Lee, J.E., Buckley, H.L., 2014. Fine-scale spatial patterns in bacterial community composition and function within freshwater ponds. *ISME J.* 8 (8), 1715–1726. <https://doi.org/10.1038/ismej.2014.21>.
- Liu, L., Yang, J., Yu, Z., Wilkinson, D.M., 2015. The biogeography of abundant and rare bacterioplankton in the lakes and reservoirs of China. *ISME J.* 9 (9), 2068–2077. <https://doi.org/10.1038/ismej.2015.29>.
- Liu, L.M., Liu, M., Wilkinson, D.M., Chen, H.H., Yu, X.Q., Yang, J., 2017. DNA metabarcoding reveals that 200-mum-size-fractionated filtering is unable to discriminate between planktonic microbial and large eukaryotes. *Molecular Ecology Resources* 17 (5), 991–1002. <https://doi.org/10.1111/1755-0998.12652>.
- Liu, L.M., Chen, H.H., Liu, M., Yang, J.R., Xiao, P., Wilkinson, D.M., et al., 2019. Response of the eukaryotic plankton community to the cyanobacterial biomass cycle over 6 years in two subtropical reservoirs. *ISME J.* 13 (9), 2196–2208. <https://doi.org/10.1038/s41396-019-0417-9>.
- Logares, R., Lindstrom, E.S., Langenheder, S., Logue, J.B., Paterson, H., Laybourn-Parry, J., et al., 2013. Biogeography of bacterial communities exposed to progressive long-term environmental change. *ISME J.* 7 (5), 937–948. <https://doi.org/10.1038/ismej.2012.168>.
- Logares, R., Audic, S., Bass, D., Bittner, L., Boutte, C., Christen, R., et al., 2014. Patterns of rare and abundant marine microbial eukaryotes. *Curr. Biol.* 24 (8), 813–821. <https://doi.org/10.1016/j.cub.2014.02.050>.
- Logares, R., Tesson, S.V., Canback, B., Pontarp, M., Hedlund, K., Rengefors, K., 2018. Contrasting prevalence of selection and drift in the community structuring of bacteria and microbial eukaryotes. *Environ. Microbiol.* 20 (6), 2231–2240. <https://doi.org/10.1111/1462-2920.14265>.
- Lynch, M.D.J., Neufeld, J.D., 2015. Ecology and exploration of the rare biosphere. *Nat. Rev. Microbiol.* 13 (4), 217–229. <https://doi.org/10.1038/nrmicro3400>.
- Magoc, T., Salzberg, S.L., 2011. FLASH: fast length adjustment of short reads to improve genome assemblies. *Bioinformatics* 27 (21), 2957–2963. <https://doi.org/10.1093/bioinformatics/btr507>.
- Mangot, J.F., Domaizon, I., Taib, N., Marouni, N., Duffaud, E., Bronner, G., et al., 2013. Short-term dynamics of diversity patterns: evidence of continual reassembly within lacustrine small eukaryotes. *Environ. Microbiol.* 15 (6), 1745–1758. <https://doi.org/10.1111/1462-2920.12065>.
- Massana, R., Pedros-Alio, C., 2008. Unveiling new microbial eukaryotes in the surface ocean. *Curr. Opin. Microbiol.* 11 (3), 213–218. <https://doi.org/10.1016/j.mib.2008.04.004>.
- Matsuzaki, S.S., Suzuki, K., Kadoya, T., Nakagawa, M., Takamura, N., 2018. Bottom-up linkages between primary production, zooplankton, and fish in a shallow, hypereutrophic lake. *Ecology* 99 (9), 2025–2036. <https://doi.org/10.1002/ecy.2414>.
- Menden-Deuer, S., Lessard, E.J., 2000. Carbon to volume relationships for dinoflagellates, diatoms, and other protist plankton. *Limnol. Oceanogr.* 45 (3), 569–579. <https://doi.org/10.4319/lo.2000.45.3.0569>.
- Moore, S.K., Trainer, V.L., Mantua, N.J., Parker, M.S., Laws, E.A., Backer, L.C., et al., 2008. Impacts of climate variability and future climate change on harmful algal blooms and human health. *Environ. Health* 7. ArtN S410.1186/1476-069x-7-S2-S4.
- Morrison-Whittle, P., Goddard, M.R., 2015. Quantifying the relative roles of selective and neutral processes in defining eukaryotic microbial communities. *ISME J.* 9 (9), 2003–2011. <https://doi.org/10.1038/ismej.2015.18>.
- Ning, D.L., Deng, Y., Tiedje, J.M., Zhou, J.Z., 2019. A general framework for quantitatively assessing ecological stochasticity. *Proc. Natl. Acad. Sci. U. S. A* 116 (34), 16892–16898. <https://doi.org/10.1073/pnas.1904623116>.
- Office of the State Oceanic Administration, 2006. Comprehensive Survey and Assessment Technique Regulations in Offshore Area of China. Marine chemistry survey technique regulations. Beijing. Ocean Press.
- Oksanen, J., Blanchet, F., Friendly, M., Kindt, R., Legendre, P., et al., 2019. *Vegan: Community Ecology Package*. R Package Version 2, pp. 5–6.
- Olesen, J.M., Bascompte, J., Dupont, Y.L., Jordano, P., 2007. The modularity of pollination networks. *Proc. Natl. Acad. Sci. U. S. A* 104 (50), 19891–19896. <https://doi.org/10.1073/pnas.0706375104>.
- Pan, Y., Yang, J., McManus, G.B., Lin, S., Zhang, W., 2019. Insights into protist diversity and biogeography in intertidal sediments sampled across a range of spatial scales. *Limnol. Oceanogr.* 65 (5), 1103–1115. <https://doi.org/10.1002/lno.11375>.
- Pawłowski, J., Esling, P., Lejzerowicz, F., Cedhagen, T., Wilding, T.A., 2014. Environmental monitoring through protist next-generation sequencing metabarcoding: assessing the impact of fish farming on benthic foraminifera communities. *Molecular Ecology Resources* 14 (6), 1129–1140. <https://doi.org/10.1111/1755-0998.12261>.
- R Core Team, 2015. R: a Language and Environment for Statistical Computing. R Foundation for Statistical Computing, Vienna, Austria. URL: <http://www.R-project.org/>.
- Rognes, T., Flouri, T., Nichols, B., Quince, C., Mahe, F., 2016. VSEARCH: a versatile open source tool for metagenomics. *PeerJ* 4. ArtN e258410.7717/peerj.2584.
- Santhanam, P., Thirunavukkarasu, A.R., Perumal, P., 2015. *Advances in Marine and Brackishwater Aquaculture*. Springer India.
- Santoferrara, L.F., 2019. Current practice in plankton metabarcoding: optimization and error management. *J. Plankton Res.* 41 (5), 571–582. <https://doi.org/10.1093/plankt/fbz041>.
- Santoferrara, L.F., Rubin, E., McManus, G.B., 2018. Global and local DNA (meta) barcoding reveal new biogeography patterns in tintinnid ciliates. *J. Plankton Res.* 40 (3), 209–221. <https://doi.org/10.1093/plankt/fby011>.
- Santoferrara, L., Burki, F., Filker, S., Logares, R., Dunthorn, M., McManus, G.B., 2020. Perspectives from ten years of protist studies by high-throughput metabarcoding. *J. Eukaryot. Microbiol.* <https://doi.org/10.1111/jeu.12813>.
- Schloss, P.D., Westcott, S.L., Ryabin, T., Hall, J.R., Hartmann, M., Hollister, E.B., et al., 2009. Introducing mothur: open-source, platform-independent, community-supported software for describing and comparing microbial communities. *Appl. Environ. Microbiol.* 75 (23), 7537–7541. <https://doi.org/10.1128/Aem.01541-09>.
- Song, X., Xu, Z., Liu, Q., Li, Y., Ma, Y., Wang, J., et al., 2016. Comparative study of the composition and genetic diversity of the picoeukaryote community in a Chinese aquaculture area and an open sea area. *J. Mar. Biol. Assoc. U. K.* 97 (1), 151–159. <https://doi.org/10.1017/s0025315416000205>.
- Stegen, J.C., Lin, X.J., Fredrickson, J.K., Chen, X.Y., Kennedy, D.W., Murray, C.J., et al., 2013. Quantifying community assembly processes and identifying features that impose them. *ISME J.* 7 (11), 2069–2079. <https://doi.org/10.1038/ismej.2013.93>.
- Vellend, M., Srivastava, D.S., Anderson, K.M., Brown, C.D., Jankowski, J.E., Kleynhans, E.J., et al., 2014. Assessing the relative importance of neutral stochasticity in ecological communities. *Oikos* 123 (12), 1420–1430. <https://doi.org/10.1111/oik.01493>.
- Wei, Z.L., You, J.G., Wu, H.L., Yang, F.F., Long, L.J., Liu, Q., et al., 2017. Bioremediation using *Gracilaria lemaneiformis* to manage the nitrogen and phosphorous balance in an integrated multi-trophic aquaculture system in Yantian Bay, China. *Mar. Pollut. Bull.* 121 (1–2), 313–319. <https://doi.org/10.1016/j.marpolbul.2017.04.034>.
- Weiss, S., Van Treuren, W., Lozupone, C., Faust, K., Friedman, J., Deng, Y., et al., 2016. Correlation detection strategies in microbial data sets vary widely in sensitivity and precision. *ISME J.* 10 (7), 1669–1681. <https://doi.org/10.1038/ismej.2015.235>.
- Williams, R.J., Howe, A., Hofmockel, K.S., 2014. Demonstrating microbial co-occurrence pattern analyses within and between ecosystems. *Front. Microbiol.* 5. ArtN 35810.3389/fmicb.2014.00358.
- Wu, W.X., Logares, R., Huang, B.Q., Hsieh, C.H., 2017. Abundant and rare picoeukaryotic sub-communities present contrasting patterns in the epipelagic waters of marginal seas in the northwestern Pacific Ocean. *Environ. Microbiol.* 19 (1), 287–300. <https://doi.org/10.1111/1462-2920.13606>.
- Wu, W.X., Lu, H.P., Sastri, A., Yeh, Y.C., Gong, G.C., Chou, W.C., et al., 2018. Contrasting the relative importance of species sorting and dispersal limitation in shaping marine bacterial versus protist communities. *ISME J.* 12 (2), 485–494. <https://doi.org/10.1038/ismej.2017.183>.
- Xie, B., Huang, J., Huang, C., Wang, Y., Shi, S., Huang, L., 2020. Stable isotopic signatures ( $\delta^{13}C$  and  $\delta^{15}N$ ) of suspended particulate organic matter as indicators for fish cage culture pollution in Sansha Bay, China. *Aquaculture* 522. <https://doi.org/10.1016/j.aquaculture.2020.735081>.
- Xiong, W., Jousset, A., Guo, S., Karlsson, I., Zhao, Q.Y., Wu, H.S., et al., 2018. Soil protist communities form a dynamic hub in the soil microbiome. *ISME J.* 12 (2), 634–638. <https://doi.org/10.1038/ismej.2017.171>.
- Xue, M., Chen, Y.Z., Tian, X., Yan, M., Zhang, Z.P., 2018a. Detection of the expansion of marine aquaculture in Sansha Bay by remote sensing. *Igarss* 7866–7869. <https://doi.org/10.1109/igarss.2018.8519028>.
- Xue, Y., Chen, H., Yang, J.R., Liu, M., Huang, B., Yang, J., 2018b. Distinct patterns and processes of abundant and rare eukaryotic plankton communities following a reservoir cyanobacterial bloom. *ISME J.* 12 (9), 2263–2277. <https://doi.org/10.1038/s41396-018-0159-0>.
- Yan, Z., Hao, Z., Wu, H., Jiang, H., Yang, M., Wang, C., 2019. Co-occurrence patterns of the microbial community in polycyclic aromatic hydrocarbon-contaminated riverine sediments. *J. Hazard Mater.* 367, 99–108. <https://doi.org/10.1016/j.jhazmat.2018.12.071>.
- Yang, J., Jiang, H.C., Wu, G., Liu, W., Zhang, G.J., 2016. Distinct factors shape aquatic and sedimentary microbial community structures in the lakes of western China. *Front. Microbiol.* 7. ArtN 178210.3389/fmicb.2016.01782.
- Yao, J., Huang, J.H., Ding, Y., Xu, Y., Xu, H., Zang, R.G., 2020. Ecological uniqueness of species assemblages and their determinants in forest communities. *Divers. Distrib.* <https://doi.org/10.1111/ddi.13205>.
- Yokoyama, H., Ishihi, Y., 2010. Bioindicator and biofilter function of *Ulva* spp. (Chlorophyta) for dissolved inorganic nitrogen discharged from a coastal fish farm - potential role in integrated multi-trophic aquaculture. *Aquaculture* 310 (1–2), 74–83. <https://doi.org/10.1016/j.aquaculture.2010.10.018>.
- Zhang, Y., Zhao, Z.H., Dai, M.H., Jiao, N.Z., Herndl, G.J., 2014. Drivers shaping the diversity and biogeography of total and active bacterial communities in the South China Sea. *Mol. Ecol.* 23 (9), 2260–2274. <https://doi.org/10.1111/mec.12739>.
- Zhang, W.J., Pan, Y.B., Yu, L.Y., Liu, L.M., 2017. Genetic diversity patterns of microeukaryotic plankton communities in Shenhui Bay, southeast China. *Continental Shelf Res.* 141, 68–75. <https://doi.org/10.1016/j.csr.2017.05.005>.
- Zhang, W.J., Pan, Y.B., Yang, J., Chen, H.H., Holohan, B., Vaudrey, J., et al., 2018. The diversity and biogeography of abundant and rare intertidal marine microeukaryotes explained by environment and dispersal limitation. *Environ. Microbiol.* 20 (2), 462–476. <https://doi.org/10.1111/1462-2920.13916>.
- Zheng, X.F., Zhang, K.K., Yang, T., He, Z.L., Shu, L.F., Xiao, F.S., et al., 2020. Sediment resuspension drives protist metacommunity structure and assembly in grass carp (*Ctenopharyngodon idella*) aquaculture ponds. *Sci. Total Environ.* <https://doi.org/10.1016/j.scitotenv.2020.142840>.
- Zhou, J.Z., Ning, D.L., 2017. Stochastic community assembly: does it matter in microbial ecology? *Microbiol. Mol. Biol. Rev.* 81 (4). ArtN e00002-1710.1128/MMBR.00002-17.
- Ziegler, M., Eguiluz, V.M., Duarte, C.M., Voolstra, C.R., 2018. Rare symbionts may contribute to the resilience of coral-algal assemblages. *ISME J.* 12 (1), 161–172. <https://doi.org/10.1038/ismej.2017.151>.